Surface structure of thin epitaxial $CoSi_2$ grown on Si(111)

F. Hellman* and R. T. Tung
AT&T Bell Laboratories, Murray Hill, New Jersey 07974-2070
(Received 5 August 1987; revised manuscript received 27 January 1988)

The surface structure of single-crystal, epitaxial, thin-film, $CoSi_2$ on Si(111) substrates has been studied by low-energy electron diffraction, Auger-electron spectroscopy, Rutherford backscattering, and transmission electron microscopy. By controlling deposition and annealing parameters, the surface may be reversibly prepared with either of two stable structures which we call "$CoSi_2$-*C*" and "$CoSi_2$-*S*." The $CoSi_2$-*C* surface appears to be a bulk termination of the $CoSi_2$ lattice with Si as the topmost layer. The $CoSi_2$-*S* surface appears to be terminated by an additional bilayer of Si which allows full coordination for all Co and Si layers. A 2×2 superstructure is seen by low-energy electron diffraction during the transition from the $CoSi_2$-*C* surface to the $CoSi_2$-*S* surface. The orientation and stability of the additional bilayer of Si at the $CoSi_2$-*S* surface may affect the orientation of epitaxial Si overlayers.

INTRODUCTION

Epitaxial silicide thin films on silicon provide the most abrupt and structurally perfect interfaces among all metal-semiconductor interfaces presently available.[1,2] The growth of epitaxial $NiSi_2$ and $CoSi_2$ under ultrahigh-vacuum (UHV) conditions on silicon substrates has been extensively studied in recent years.[3–11] Interest in these structures has stemmed from the hope that their extraordinary perfection can provide model metal-semiconductor junctions to solve fundamental scientific problems, such as the Schottky-barrier issue.[12,13] There has also been considerable interest due to the possibility of high-speed devices based on heterostructures of epitaxial silicides.[14–16] $NiSi_2$ and $CoSi_2$ are metallic and form in the CaF_2 structure with lattice parameters within 0.4% and 1.3%, respectively, of that of Si. There are known to be two epitaxial orientations of the silicide on Si(111), type *A* and type *B*. Type-*A* silicide has the same orientation as the silicon substrate; type-*B* silicide shares the surface normal [111] axis with the Si, but is rotated 180° about this axis with respect to the substrate.[6,5] It is generally observed that $CoSi_2$ forms as a type-*B* silicide.[5] However, depending on the details of the preparation conditions, double-positioned films may result due to a mixture of type-*A* and -*B* silicides.

The surface structure of $CoSi_2$ is of considerable scientific interest from the standpoint of understanding the chemical bonding in the silicide. It is also of technological importance because it is likely to affect the growth of subsequent epitaxial layers. Different structures of the $CoSi_2$(111) surface have been considered in the literature: relaxed bulk-terminated with either Si or Co as the top layer of atoms and terminated by an additional Si bilayer.[17–19] Pirri *et al.* found a transition with annealing temperature between two different surface structures with different low-energy electron diffraction (LEED) patterns, work functions, and angle-resolved ultraviolet photoemission spectra.[17] They suggested that the low-temperature surface was bulk-terminated with Co as the top layer. The surface produced with higher-temperature anneals was proposed to be, except for surface relaxations, a termination of the $CoSi_2$ lattice at a position such as to leave two Si layers at the surface. This structure has two layers of Si more than the proposed low-temperature surface. Chambers *et al.* have studied ultrathin $CoSi_2$ islands on Si(111) with careful angle-resolved Auger analysis and observed only one surface structure.[18] They showed that this surface was not a bulk termination of the $CoSi_2$ lattice: it consisted instead of an additional Si bilayer on top of the bulk $CoSi_2$, resulting in a surface with the top *three* atomic planes being occupied by Si.[18] Wu *et al.* found one surface which they determined from a LEED study to be a bulk-terminated surface with a single Si layer at the surface.[19] They also found that a higher-temperature anneal produced what they termed a "post-silicide phase" which showed a different LEED pattern than the bulk-terminated surface and unclear Auger results. They did not determine the structure of this post-silicide phase. The four proposed models for the $CoSi_2$(111) surface thus are not in agreement with one another.

These previous surface studies examined thin epitaxial layers grown by deposition and annealing of Co on Si(111) substrates. This technique produces $CoSi_2$ films with primarily type-*B* orientation, but often a substantial fraction of the film possesses a type-*A* orientation. Furthermore, pinholes, the size and density of which depends critically on processing, also occupy a non-negligible fraction of the surface. Pinholes and the mixture of type-*A* and type-*B* crystals complicate the study of surface structures. For instance, the usefulness of LEED characteristics in revealing the surface structure is greatly reduced when comparable amounts of *A* and *B* grains are present. Strong threefold LEED patterns associated with a unique structure can easily turn into sixfold symmetric patterns due to a mixture of *A* and *B* orientations. Pinholes and other morphology can dominate the

Auger electron spectroscopy (AES) signal and make the results not representative of the $CoSi_2$ surface under study. These problems are not insurmountable, as an independent structural characterization, such as transmission electron microscopy (TEM), can remove most of the difficulties in data analyses. However, in practice, such accompanying analyses of the layer morphology have not been reported along with surface studies of thin epitaxial silicides.

In this paper, we present results of an investigation into the surface structures of the $CoSi_2(111)$. The $CoSi_2$ layers used in this study have been experimentally demonstrated to be near-perfect, uniform, single-crystal, type-*B* oriented stoichiometric, $CoSi_2$. Clear evidence for the existence of two quasistable 1×1 surface structures, "$CoSi_2$-*C*" and "$CoSi_2$-*S*", is presented and their characteristics documented. A 2×2 structure is shown to occur during the transition between these two surface structures. Experiments using deposition of monolayer(s) of Co or Si on these two surfaces have unambiguously shown that the difference between the two is an additional Si bilayer on the $CoSi_2$-*S* structure, as found by Pirri *et al.*[17] The single-crystal nature of the silicide films, however, allows us to draw more concrete, and slightly different, conclusions as to the structure of these surfaces. In particular, the LEED patterns of one of the surfaces, the $CoSi_2$-*C*, match calculations for bulk-terminated $CoSi_2$ with Si as the top layer.[19] A model originally proposed for $CoSi_2$ clusters will be shown to be the likely structure for the $CoSi_2$-*S* surface.[18] The merits of this structure, which allows full coordination for all atoms, will be discussed. Furthermore, the influence of the surface structure of $CoSi_2(111)$ on the subsequent growth of epitaxial Si is discussed. The particular structure of the $CoSi_2$-*S* surface allows us to suggest an explanation for the observation that heterostructures of $Si_{sub}/CoSi_2/Si_{over}$ usually have *ABB* orientation on (111) substrates.[20,21] [This is surprising because the predominance of type-*B* orientation observed for $CoSi_2$ thin layers on Si(111) ordinarily would imply the dominance of this orientation at the interface between the Si overlayer and $CoSi_2$, and therefore an *ABA* orientation.] The development of the $CoSi_2$-*S* surface structure also has been found to have an influence on the $CoSi_2$ layer morphology.

EXPERIMENTAL PROCEDURES

Samples were prepared in a bakeable UHV chamber with a base pressure of 1×10^{-10} Torr. Polished (111)-oriented *p*-type (boron-doped, 0.6 Ω-cm) Si substrates were degreased and then cleaned by repeated chemically induced growth and removal of an oxide layer. The final step is growth of a volatile oxide layer which protects the Si surface during transfer to the growth chamber.[22] This oxide layer is removed prior to deposition by raising the substrate temperature to ~820 °C for ~30–60 sec. The resulting Si surface shows a sharp 7×7 LEED pattern and AES analysis shows no sign of C or O contamination. Co or Si was deposited by electron-beam evaporation at rates of 0.5–1.0 Å/sec. The pressure in the chamber remained below 2.5×10^{-10} Torr during deposition. The substrate temperature was below 50 °C for all depositions described in this paper. Samples were then annealed *in situ* by resistive heating of the substrate. Examination of the resulting structures by LEED and AES were also accomplished *in situ*. No sign of C or O contamination was found after annealing. Rutherford backscattering spectrometry (RBS) and TEM analyses were performed *ex situ* on the silicide samples.

EXPERIMENTAL RESULTS

The approach taken was first to grow a uniform silicide "substrate" which is single crystal and practically pinhole-free. Deposition of *both* Co and Si has been shown to produce epitaxial $CoSi_2$ films far superior in crystallinity and layer uniformity than those grown with deposition of only Co.[20,21] TEM has found these films to be very uniform with a negligible amount of pinholes and to have a type-*B* orientation.[20] An example is shown in Fig. 1 which is a plan-view, (220) bright-field TEM image of a ~70-Å-thick $CoSi_2$ substrate layer. This layer was grown by deposition of 20 Å of Co followed immediately by 40 Å of Si and annealed at ~580 °C for 1 min. Moiré fringes and a relatively uniform array of misfit dislocations are clearly visible and indicate that the $CoSi_2$ layer is uniform and contains a very low density of pinholes. Dark-field imaging with a diffracted beam specific to a type-*B* orientation shows that the entire layer has the type-*B* orientation. RBS random and [111] channeling spectra of a typical thin $CoSi_2$ layer are shown in Fig. 2. A glancing exit angle was used to increase the depth reso-

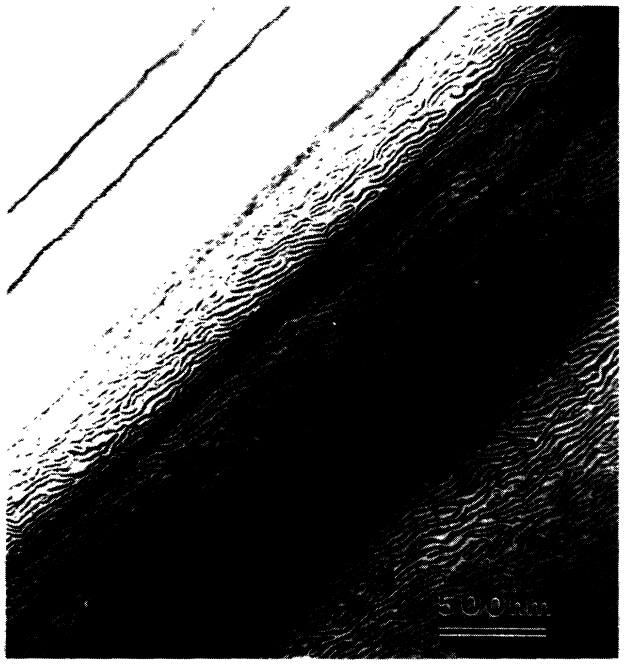

FIG. 1. Plan-view (220) two-beam bright-field TEM image of a ~70-Å-thick $CoSi_2$ "substrate" layer. The dark bands crossing the figure diagonally are thickness fringes.

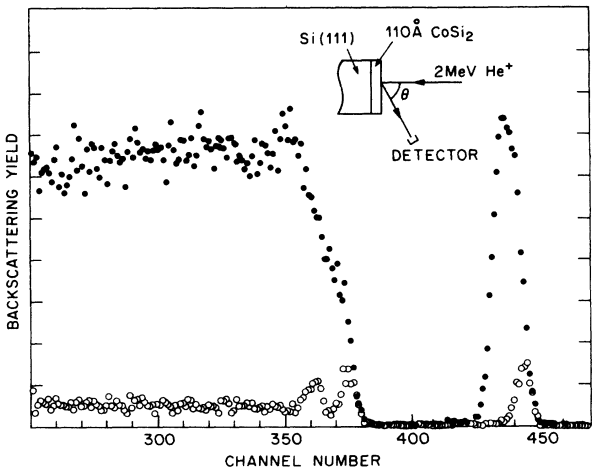

FIG. 2. Channeling and random Rutherford backscattering spectra of a ~80-Å type-*B* $CoSi_2$ layer grown by deposition of Co and Si on Si(111). A glancing exit angle, $\theta = \sim 84°$, was used to take these spectra.

lution. A channeling minimum yield χ_{min} of less than 3% was measured for this silicide layer, indicating excellent crystallinity. The channeling peak at the $CoSi_2$/Si interface has been observed previously.[23,24] The origin of this peak is discussed elsewhere.[25]

After a uniform $CoSi_2$ substrate is grown, the structure of its surface is studied by LEED and AES. Two distinctly different 1×1 surfaces, "$CoSi_2$-*C*" and "$CoSi_2$-*S*," have been observed for $CoSi_2$ layers. (The postscripts "*C*" and "*S*" stand, respectively, for "Co-rich" and "Si-rich.") TEM and RBS show that both structures occur on uniform, *B*-oriented, stoichiometric, $CoSi_2$ layers. Usually, the starting silicide surface displays a $CoSi_2$-*S* structure, if the growth of the "silicide substrate" involves heating to above ~550 °C. However, we have also used different preparation conditions which produced a $CoSi_2$-*C* structure as the starting surface. For example, deposition of ~10 Å Co followed by ~20 Å Si at room temperature and annealing to ~500 °C for 1–2 min generally results in a uniform, *B*-oriented $CoSi_2$ substrate with a $CoSi_2$-*C* surface. Deposition of monolayer(s) of Co or Si on the $CoSi_2$ substrates and annealing then allows the observation of various transitions of the surface structures as described below.

Normal incident, reverse-viewed, LEED patterns of the two 1×1 surfaces are shown in Figs. 3 and 4. The LEED characteristics of the $CoSi_2$-*C* surface, shown in Fig. 3, include a strong asymmetry in the (10)- and (01)-type beams at ~57 and 86 eV.[26] For a pure type-*B* oriented $CoSi_2$ layer, the (10) LEED beams are intense at ~57 eV, while the (01)-type beams are almost nonexistent. Another strong threefold pattern is observed at ~86 eV. However, the intensities of the two types of beams are reversed, the (10)-type beams becoming very dim. Selected LEED patterns of a $CoSi_2$-*S* surface are shown in Fig. 4. They are entirely different from the patterns of the $CoSi_2$-*C* surface, as can be seen from a comparison of Figs. 3 and 4. A $CoSi_2$-*S* surface on a type-*B* oriented silicide layer shows strong (10)-type diffracted beams and weak (01) beams at ~80 eV. At ~46 eV, a reversal of the intensities of these two types of beams is observed. A double-path cylindrical mirror analyzer was used to record the AES peak heights. Auger analysis was performed using normal incident 3-kV electrons with ~4 eV modulations. Table I shows the peak height ratios (unnormalized) of the Co *MNN* (53-eV) and Si *LMM* (92-eV) and the Co *LMM* (775-eV) and Si *KLL* (1619-eV) lines for different surface conditions. The higher-energy lines (775 and 1619 eV) have longer electron mean free paths, ~12–20 Å, and therefore their ratios give a better indication of the composition of the silicide. Ratios of the lower-energy lines are more surface "sensitive," because of shorter mean free paths, ~5 Å. Table I shows that the $CoSi_2$-*C* surface has a ratio of ~0.24 for the surface-sensitive transitions and ~2.9 for the higher-energy peaks. The $CoSi_2$-*S* surface shows a peak height

TABLE I. Unnormalized Auger peak height ratios for $CoSi_2$ under various treatments as shown. The ratios of the lower-energy Co *MNN* (53-eV) and Si *LMM* (92-eV) lines are more surface-sensitive than the ratios of the Co *LMM* (775-eV) and Si *KLL* (1619-eV) lines, thus the ratios of the higher-energy lines reflect the material further from the surface.

Surface preparation			Surface characteristics		
Deposition (ML)	"Substrate"	Anneal temperature and time	Surface type (from LEED)	Peak Height ratios (Co *MNN*):(Si *LMM*)	(Co *LMM*):(Si *KLL*)
			$CoSi_2$-*C*	0.24±0.015	2.9±0.2
			$CoSi_2$-*S*	0.095±0.015	2.7±0.2
~1 ML Si	$CoSi_2$-*C*	none	mixed	0.12	2.5
~2 ML Si	$CoSi_2$-*C*	none	diffuse $CoSi_2$-*S*	0.07	2.5
~3 ML Si	$CoSi_2$-*C*	none	dim	0.06	2.3
~1 ML Si	$CoSi_2$-*C*	450 °C/1 min	mixed	0.13	2.7
~2 ML Si	$CoSi_2$-*C*	450 °C/1 min	$CoSi_2$-*S*	0.085	2.6
~3 ML Si	$CoSi_2$-*C*	450 °C/1 min	$CoSi_2$-*S*	0.075	2.6
~0.5 ML Co	$CoSi_2$-*S*	none	mixed	0.17	2.8
~1 ML Co	$CoSi_2$-*S*	none	diffuse $CoSi_2$-*C*	0.30	3.3
~0.5 ML Co	$CoSi_2$-*S*	450 °C/1 min	mixed	0.19	2.9
~1 ML Co	$CoSi_2$-*S*	450 °C/1 min	$CoSi_2$-*C*	0.25	3.3

ratio near 0.095 for the more surface-sensitive peaks and a ratio near ~2.7 for the higher-energy peaks. These numbers strongly suggest that the layer compositions are similar for the two surface structures, but the "surface composition" (of the top ~4–6 monolayers) for a $CoSi_2$-*S* structure is richer in Si than for a $CoSi_2$-*C* structure.

When a $CoSi_2$ layer with a $CoSi_2$-*C* surface is annealed for a long time (> 14 min) at ~520 °C or when it is annealed at a higher temperature (> 550 °C) for ~1–2 min a $CoSi_2$-*S* structure is seen on the surface. A 2×2 reconstructed surface is sometimes seen in the middle of the transition from a $CoSi_2$-*C* to a $CoSi_2$-*S* structure. This intermediate surface is most easily seen when a low annealing temperature (< ~500 °C) is used and when the initial $CoSi_2$-*C* structure is cobalt-rich as explained below. The ratio of the surface-sensitive Auger transitions for the 2×2 is between the values for the $CoSi_2$-*C* and $CoSi_2$-*S* structures.

Deposition of Si on a $CoSi_2$-*C* surface also leads to a $CoSi_2$-*S* surface. LEED patterns at 78 and 87 eV, the voltages most descriptive of the two $CoSi_2$ surfaces, are shown in Fig. 5 before and after deposition of 1 and 2 monolayers (ML) of Si onto the $CoSi_2$-*C* surface. The LEED patterns after a 2-ML Si deposition show the threefold symmetry of the $CoSi_2$-*S* surface seen in Fig. 4 *even without annealing*. Auger analysis (Table I) shows a surface stoichiometry which closely resembles that of the $CoSi_2$-*S* surface. A short (30–60 sec) anneal at 450 °C sharpened the diffraction spots and allowed a characteristic $CoSi_2$-*S* surface to appear. The LEED patterns of the

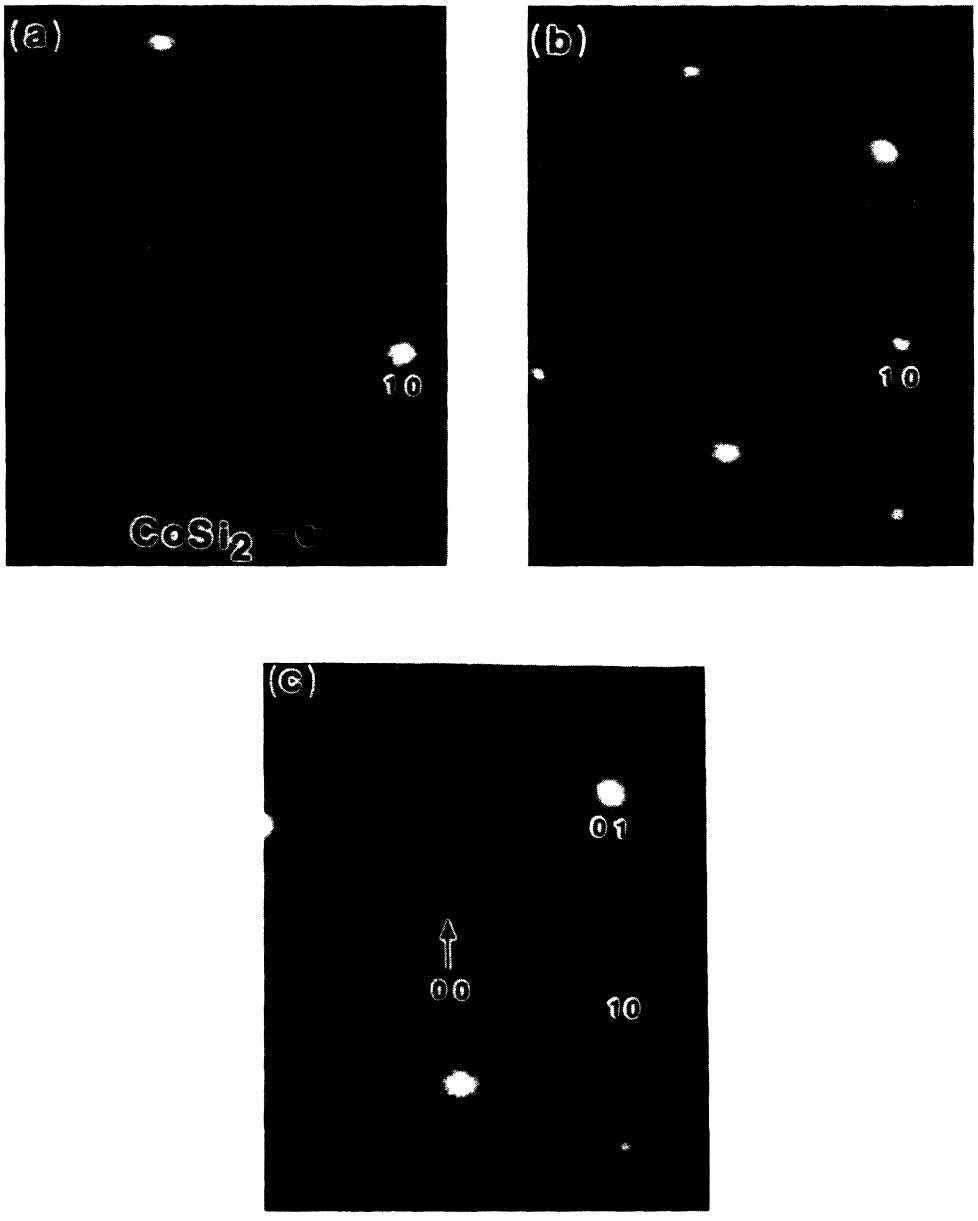

FIG. 3. LEED patterns for the $CoSi_2$-*C* surface at various energies. (a) 57 eV, (b) 79 eV, (c) 86 eV.

1 ML overcoat, even after an anneal at 450 °C, show no strong threefold symmetry at any energy. The patterns at 78 and 87 eV are not characteristic of either surface type—the surface probably contains domains of the two individual structures. After an anneal at 540 °C the $CoSi_2$-*C* surface is converted to a $CoSi_2$-*S* surface, with or without any deposited Si. Depositing 1, 2, or 4 ML of Si onto the $CoSi_2$-*S* surface causes the surface to be further Si-enriched. Annealing at low *T* reduces this excess. After annealing at 540 °C for 30 sec, LEED and AES show the surface to again be the $CoSi_2$-*S* structure. Extra Si was found from a TEM experiment to conglomerate into small islands exposing the $CoSi_2$-*S* structure between islands.

The $CoSi_2$-*S* surface can be converted to the $CoSi_2$-*C* surface by deposition of cobalt. Deposition of ~1 ML Co at room temperature on a $CoSi_2$-*S* surface results in a diffuse 1×1 $CoSi_2$-*C* structure on the surface. The Auger ratios measured after the 1 ML Co deposition are similar to those for the $CoSi_2$-*C* surface. When more than ~2 ML Co are deposited, the surface LEED patterns become very dim and diffuse. Deposition of ~0.5 ML Co on a $CoSi_2$-*S* surface results in a surface with mixed $CoSi_2$-*S* and slightly disordered $CoSi_2$-*C* domains, characterized by bright and broad (01)-type beams at ~87 eV and bright and sharp (10)-type beams at ~79 eV. With more than ~1 ML Co (up to ~10 ML) deposited on a $CoSi_2$-*S* surface, a short anneal at ~450 °C leads to a sharp $CoSi_2$-*C* LEED pattern. AES results of a surface after such an anneal are those of the $CoSi_2$-*C* substrate. Small variations in the details of the $CoSi_2$-*C* LEED pattern have been noticed which correlate with the surface stoichiometry measured by AES. For example, for a Co-rich $CoSi_2$-*C* surface (with an AES ratio of ~0.27), the most pronounced asymmetry in the LEED pattern, i.e., when the (10)-type beams reach their minimum intensity, occurs at ~89–90 eV instead of the more customary ~87 eV. On a Si-rich $CoSi_2$-*C* surface (with an AES ratio of ~0.21), the minimum intensity occurs at lower energy, ~84 eV. There are other minor changes of the LEED characteristics with stoichiometry.

A typical sequence of the transitions, back and forth, between the $CoSi_2$-*S* and $CoSi_2$-*C* structures can be found in Fig. 6. LEED patterns at characteristic energies are shown in chronological order. Figure 6(a) shows the $CoSi_2$-*S* substrate surface. Figures 6(b)–6(f) were taken after a ~2 ML Co deposition followed by anneals at the temperatures and for the times given in the caption. The first clear pattern is a threefold 1×1 $CoSi_2$-*C* structure, as the very strong asymmetry at 85 eV [seen in Fig. 6(b)] reveals. Annealing a longer time (or at slightly higher temperature) causes the pattern to change to the more complex $2\times2+1\times1$; LEED patterns at two voltages are shown. The 1×1 is now not strongly asymmetric at any

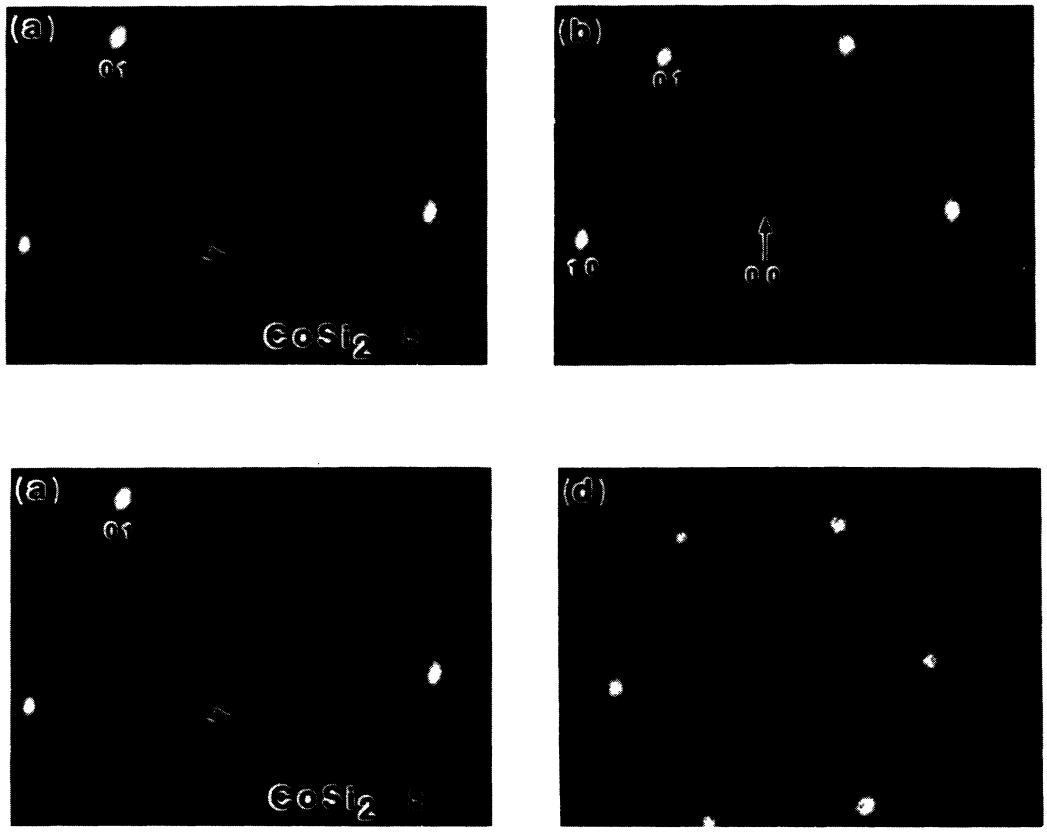

FIG. 4. LEED patterns for the $CoSi_2$-*S* surface at various energies. (a) 46 eV, (b) 58 eV, (c) 80 eV, (d) 88 eV.

voltage. Finally, the 2×2 vanishes and we are left in Fig. 6(f) with a threefold 1×1 pattern identical to that of the original $CoSi_2$-*S* substrate.

DISCUSSION

The LEED patterns of the $CoSi_2$-*C* surface are remarkably similar to the reported patterns of the $NiSi_2$ surface,[27,28] at all incident electron energies. In the case of $NiSi_2(111)$, the observed variation of LEED beam intensity as a function of energy agrees well with a calculation for a relaxed, bulk-terminated surface with Si as the topmost layer.[28] Other models such as that with the metal atom as the topmost layer[28] do not match the LEED intensity curves observed for the $NiSi_2$. Although recently there has been an issue raised about the uniqueness of the $NiSi_2$ surface structure,[29] the bulk-terminated surface structure is believed to be correct for $NiSi_2(111)$ under the reported preparation conditions.[27,28] Because of the similarity with the stable $NiSi_2(111)$, the $CoSi_2$-*C* surface thus appears to be a bulk-terminated surface with Si as the top layer, as shown in Fig. 7(a), in agreement with the conclusion of Wu *et al.*[19] The exact surface relaxation still remains to be studied.

The $CoSi_2$-*S* surface is known from AES analyses to be richer in silicon than the $CoSi_2$-*C* surface. Adding two additional layers of Si to the $CoSi_2$-*C* surface without annealing gave normalized Auger peak height ratios and

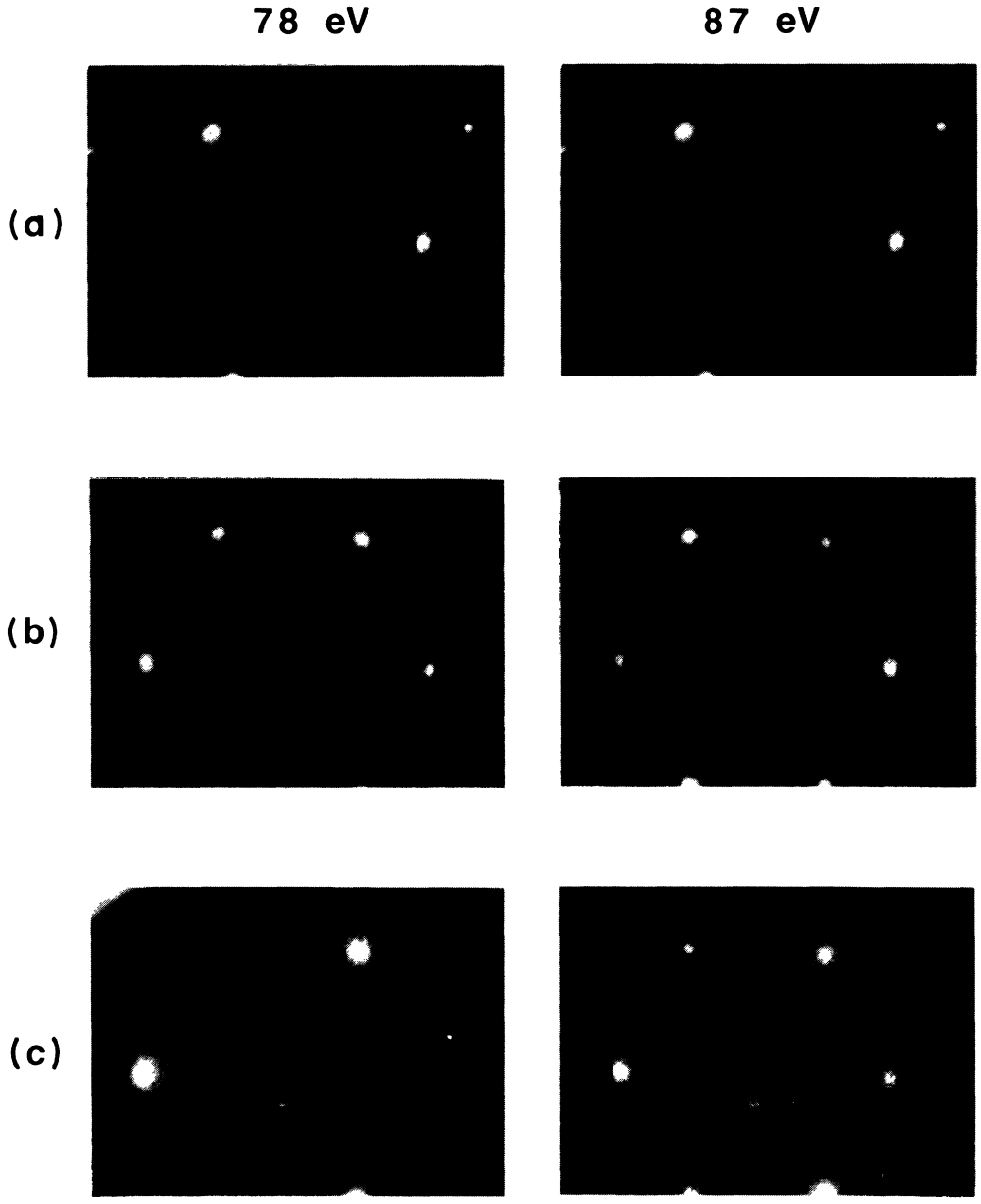

FIG. 5. LEED patterns for (a) $CoSi_2$-*C* surface (b) with one monolayer and (c) with two monolayers of Si deposited over and not annealed. Characteristic energies of the $CoSi_2$-*S* and $CoSi_2$-*C* surfaces (78 and 87 eV) are shown for each.

LEED patterns identical to those of the $CoSi_2$-*S* surface. On the other hand, one monolayer of cobalt deposited on a $CoSi_2$-*S* surface results in a $CoSi_2$-*C* surface. These results strongly suggest that the $CoSi_2$-*S* surface possesses an additional Si bilayer over the $CoSi_2$-*C* surface. The possibility that this excess Si resides below the surface layer can be ruled out from analysis of the AES results based on the electron escape depths. The dramatic difference between the LEED characteristics of the $CoSi_2$-*C* surface and that of the $CoSi_2$-*S* surface also suggests that the additional Si resides on top of the $CoSi_2$-*C* surface.

Possible arrangements of the topmost Si bilayer on the $CoSi_2$-*S* surface are shown in Figs. 7(b)–7(e). No relaxation is assumed. Models (b) and (c) assume an eightfold coordination for the topmost Co layer, the same coordination cobalt atoms have in bulk $CoSi_2$. Models (d) and (e) assume a sevenfold coordination. The stacking sequence of the Si bilayer is the same as the silicide in models (b) and (d). In models (c) and (e), the stacking sequence of the Si bilayer is reversed from that of the silicide. If Si were grown on top of these possible surfaces with the same stacking sequence as the topmost Si bilayer, type-*A* interfaces would be formed on top of (b)

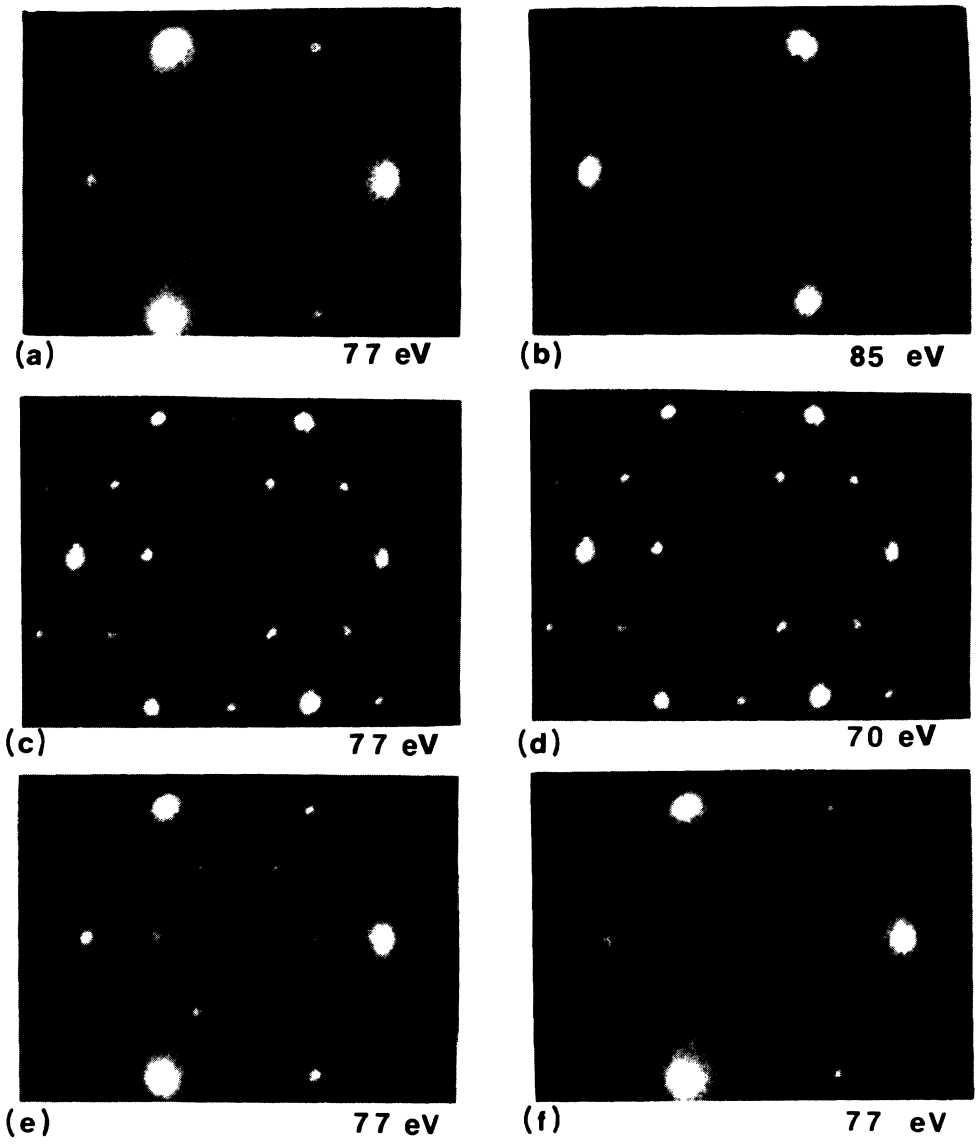

FIG. 6. LEED patterns of the $CoSi_2$ surface taken in a single deposition and annealing sequence. Voltages are as shown. (a) Silicide substrate showing strong threefold symmetry characteristic of single-crystal, epitaxial, type-*B* silicide after annealing at 580 °C for 1 min ($CoSi_2$-*S* surface). (b)–(f) show surface with 2 Å Co overlayer. (b) Annealed at 450 °C for 1 min. LEED pattern is typical of $CoSi_2$-*C* surface. (c) and (d) Annealed at 450 °C for 18 min. Patterns show 2×2 plus sixfold 1×1 symmetry. (e) Annealed at 480 °C for 9 min. Pattern shows weak 2×2 plus primarily threefold 1×1 symmetry. (f) Annealed at 590 °C for 30 sec. The LEED pattern is again typical of the $CoSi_2$-*S* surface.

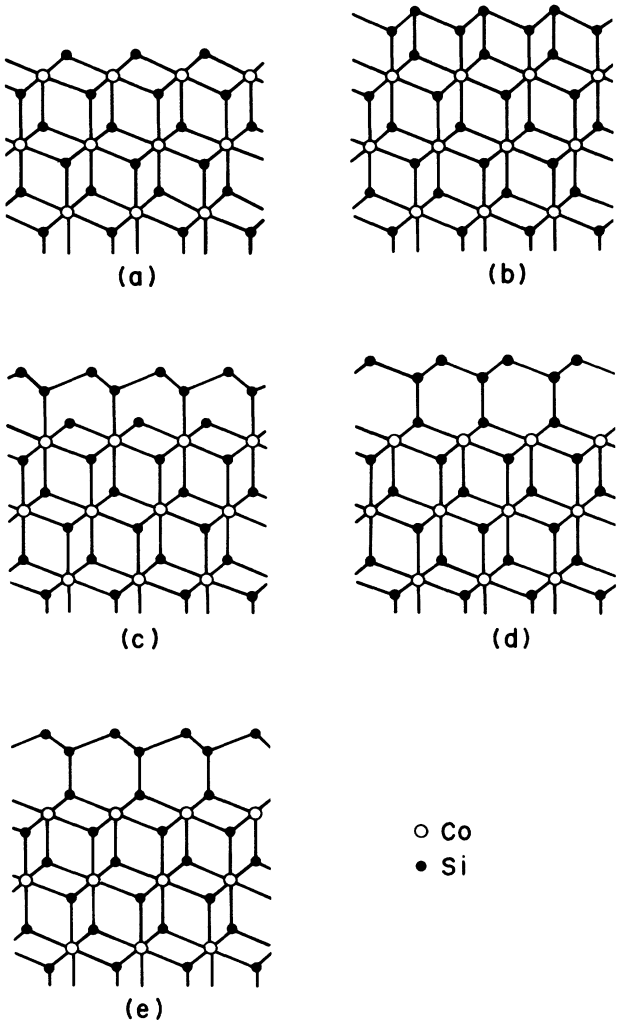

FIG. 7. Five possible models for the surface structure of $CoSi_2$. (a) Bulk-terminated. (b)–(e) Si-bilayer overlayer. Models (b) and (c) assume an eightfold coordination for the topmost Co layer. Models (d) and (e) assume a sevenfold coordination for the topmost Co layer. The Si bilayer has a type-*A* orientation with respect to the silicide in (b) and (d) and type-*B* in (c) and (e).

and (d), and type-*B* interfaces would be formed on (c) and (e). In models (d) and (e), the Si is tetravalently coordinated in the last layer of silicide but the top layer in the bilayer is missing a bond. In model (c), the top Si layer of both the Si bilayer and the silicide are missing a bond. In model (b), all Si atoms have four bonds; the bond angles of the top layer of the Si bilayer, however, are not tetrahedral. This arrangement is very similar to that of the adatom bonds on the 7×7 reconstruction of pure Si(111).[30] Because of the absence of broken bonds, model (b) is likely to be energetically favored over the other structures in Fig. 7. This conclusion is supported by the angle-resolved Auger analysis of Chambers *et al.*[18] Calculations of LEED spectra for these various surfaces could confirm the model. Actual surface energy would, of course, be greatly influenced by the amount of surface relaxation. $CoSi_2$-*S* is the equilibrium structure at the surface of $CoSi_2$. TEM evidence, presented elsewhere, shows that the transition from the $CoSi_2$-*C* to the $CoSi_2$-*S* structure is accompanied by, and may in fact cause, the pinholes so universally observed in epitaxial $CoSi_2$(111) thin films.[31] Furthermore, the Si bilayer may be present at the type-*B* $CoSi_2$/Si(111) interface, leading to an eightfold-coordinated interface with a layer of "faulted" Si.[25]

The structure of the 2×2 surface is not clear at this time. A 2×2 structure has been reported by Pirri *et al.*[17] when thin Co layers (less than 1 ML) were annealed at 600 °C. D'Avitaya *et al.*[32] and Yang *et al.*[28] also reported observation of 2×2 reconstructions (or three domains of 2×1) immediately preceding the observation of 1×1 $CoSi_2$ for thick (33-Å) Co films annealed near 600 °C. It is likely that the intermediate 2×2 structure in our experiments is the same as those previously reported. It is possible that the 2×2 structure is a superstructure of Si formed prior to forming the bilayer structure of the $CoSi_2$-*S* surface. It should be pointed out that there is more than one surface which exhibits 2×2 symmetry in the Co/Si(111) system. The 2×2 pattern shown in Fig. 5, which is seen in our experiment as the intermediate stage in the transition from a $CoSi_2$-*C* to a $CoSi_2$-*S* structure, is different from another 2×2 LEED pattern which is associated with a strained $CoSi_2$(111) surface where a reversible 2×2 to 1×1 transition is observed at ~100 °C.[25]

When further layers of Si are added to any of the Si-bilayer structures shown in Figs. 7(b)–7(e), the bonding situation changes. The energy cost of model (b) with additional layers of Si is due to the fivefold coordination of one Si layer and the missing bond of the topmost Si layer. The energy cost of model (c) with additional layers is due to two missing Si bonds. The cost to (d) and (e) with Si overlayers is due to one missing Co and one missing Si bond. Local-density-functional calculations show model (c) to have the lowest energy of the four.[33] However, model (b) *as shown* (without any additional layers of Si) should be energetically more favorable still, suggesting an explanation for the observation made above that when thin Si layers are deposited on the $CoSi_2$-*S* surface and annealed, this extra Si conglomerates into small islands, exposing the $CoSi_2$-*S* structure in between.

Epitaxial overlayers of Si may be grown by depositing a 20-Å layer of Si at room temperature onto a $CoSi_2$-*S* surface and annealing (the so-called "template" method).[20,21] This Si layer has a type-*A* orientation with respect to the silicide layer. This orientation is surprising, since a type-*B* orientation between silicide and Si substrate is observed to be strongly preferred. We suggest that the explanation lies in the orientation of the bilayer; in model (b), the bilayer has a type-*A* orientation with respect to the silicide. Subsequent Si layers are then grown epitaxially onto this bilayer. The explanation of the observed asymmetry in interface type for Si(substrate)-silicide-Si structures may lie simply in the inability of the Si overlayers to reorient from the atomic positions of model (b) into the energetically more favorable structure of a type-*B* $CoSi_2$/Si interface.

CONCLUSIONS

As discussed above, the contribution of this work is an accurate documentation of the surface structures associated with $CoSi_2$, made possible by the detailed characterization of the layer structure of the epitaxial $CoSi_2$ which is shown to be uniform and single crystalline. LEED and Auger analysis have clearly identified a transition between two different 1×1 surfaces: the "$CoSi_2$-*C*" and the "$CoSi_2$-*S*." The $CoSi_2$-*C* structure appears to be a bulk-terminated structure with Si as the top layer. The $CoSi_2$-*S* structure seems to agree with the incorporation of an additional Si bilayer. The Si bilayer appears to have an *A*-type orientation with respect to the silicide, suggesting an explanation for the observation that overlayers of Si grow in the same orientation as the silicide. The possibility of altering the orientation of epitaxial Si layers grown over the $CoSi_2$ by manipulating the surface structure of the $CoSi_2$ is currently being investigated.[31]

ACKNOWLEDGMENTS

The authors would like to thank J. L. Batstone for TEM analyses and D. Bahnck for sample preparation. We are indebted to D. R. Hamann and H.-J. Gossmann for useful discussions on surface models.

---

*Present address: Department of Physics, The University of California at San Diego, La Jolla, CA 92093.

[1]D. Cherns, G. R. Anstis, J. L. Hutchison, and J. C. H. Spence, Philos. Mag. A **46**, 849 (1982).

[2]J. M. Gibson, J. C. Bean, J. M. Poate, and R. T. Tung, Appl. Phys. Lett. **41**, 818 (1982).

[3]J. C. Bean and J. M. Poate, Appl. Phys. Lett. **37**, 643 (1980).

[4]S. Saitoh, H. Ishiwara, and S. Furukawa, Appl. Phys. **37**, 203 (1980).

[5]R. T. Tung, J. M. Gibson, J. C. Bean, J. M. Poate, and D. C. Jacobson, Appl. Phys. Lett. **40**, 684 (1982).

[6]R. T. Tung, J. M. Gibson, and J. M. Poate, Phys. Rev. Lett. **50**, 429 (1983).

[7]A. Ishizaka and Y. Shiraki, Jpn. J. Appl. Phys. **23**, L499 (1984).

[8]Y. C. Kao, M. Tejwani, Y. H. Xie, T. L. Lin, and K. L. Wang, J. Vac. Sci. Technol. B **3**, 596 (1985).

[9]E. J. van Loenen, A. E. M. J. Fischer, J. F. van der Veen, and F. LeGoues, Surf. Sci. **154**, 52 (1985).

[10]C. D'Anterroches and F. Arnaud D'Avitaya, Surf. Sci. **137**, 351 (1986).

[11]B. D. Hunt, N. Lewis, E. L. Hall, L. G. Turner, L. J. Schowalter, M. Okamoto, and S. Hashimoto, Mater. Res. Soc. Symp. Proc. **56**, 151 (1986).

[12]R. T. Tung, Phys. Rev. Lett. **52**, 461 (1984).

[13]M. Liehr, P. E. Schmidt, F. K. LeGoues, and P. S. Ho, Phys. Rev. Lett. **54**, 2139 (1985).

[14]E. Rosencher, S. Delage, Y. Campidelli, and F. Arnaud D'Avitaya, Electron. Lett. **20**, 762 (1984).

[15]R. T. Tung, A. F. J. Levi, and J. M. Gibson, Appl. Phys. Lett. **48**, 635 (1986).

[16]B. D. Hunt, L. J. Schowalter, and R. M. Chrenko (unpublished).

[17]C. Pirri, J. C. Peruchetti, D. Bolmont, and G. Gewinner, Phys. Rev. B **33**, 4108 (1986).

[18]S. A. Chambers, S. B. Anderson, H. W. Chen, and J. H. Weaver, Phys. Rev. B **34**, 913 (1986).

[19]S. C. Wu, Z. Q. Wang, Y. S. Li, F. Jona, and P. M. Marcus, Phys. Rev. B **33**, 2900 (1986).

[20]R. T. Tung, A. F. J. Levi, and J. M. Gibson, Appl. Phys. Lett. **48**, 635 (1986).

[21]B. D. Hunt, N. Lewis, L. J. Schowalter, E. L. Hall, and L. G. Turner, Mater. Res. Soc. Symp. Proc. **77**, 351 (1987).

[22]A. Ishizaka and Y. Shiraki, J. Electrochem. Soc. **133**, 666 (1986).

[23]R. T. Tung, F. Hellman, J. M. Gibson, and T. Boone, Mater. Res. Soc. Symp. Proc. **91**, 451 (1987).

[24]D. N. Jamieson, G. Bai, Y. C. Kao, C. W. Nieh, M.-A. Nicolet, and K. L. Wang, Mater. Res. Soc. Symp. Proc. **91**, 473 (1987).

[25]R. T. Tung, J. L. Batstone, and S. M. Yalisove, J. Electrochem. Soc. (to be published).

[26]Note that the 2D unit-cell convention of E. A. Wood, J. Appl. Phys. **35**, 1306 (1964), has been adopted. The (10) and the (01) LEED beams are equivalent to $\mathbf{g}=\frac{1}{3}(4,-2,-2)$ and $\mathbf{g}=\frac{1}{3}(2,-4,2)$, respectively, in bulk diffractions. To avoid confusion, LEED beams are labeled according to crystal orientation of the Si substrate.

[27]R. T. Tung, J. Vac. Sci. Technol. A **5**, 1840 (1987).

[28]W. S. Yang, F. Jona, and P. M. Marcus, Phys. Rev. B **28**, 7377 (1983).

[29]V. Hinkel, L. Sorba, H. Haak, K. Horn, and W. Braun, Appl. Phys. Lett. **50**, 1257 (1987).

[30]K. Takayanagi, Y. Tanishiro, M. Takahashi, and S. Takahashi, J. Vac. Sci. Technol. A **3**, 1502 (1985).

[31]R. T. Tung and J. L. Batstone, Appl. Phys. Lett. **52**, 648 (1988).

[32]F. Arnaud D'Avitaya, S. Delage, E. Rosencher, and J. Derrien, J. Vac. Sci. Technol. B **3**, 770 (1985).

[33]D. R. Hamann, Phys. Rev. Lett. **60**, 313 (1988).

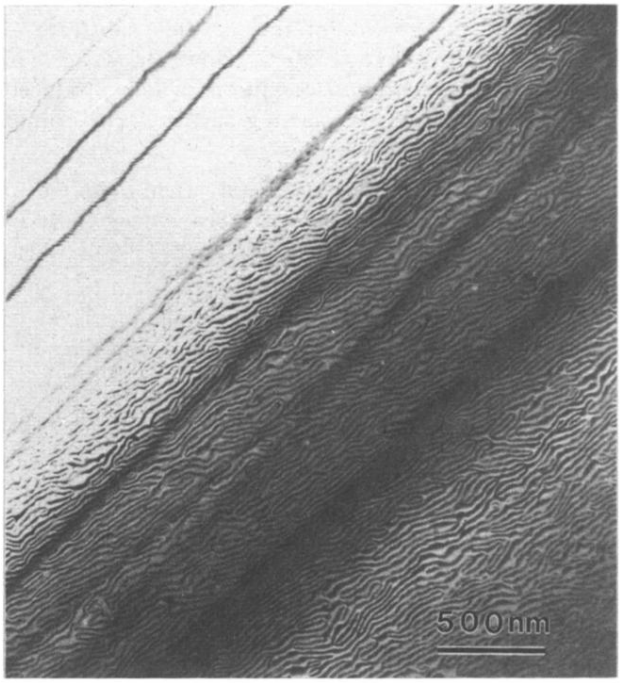

FIG. 1. Plan-view (220) two-beam bright-field TEM image of a $\sim$70-Å-thick $CoSi_2$ "substrate" layer. The dark bands crossing the figure diagonally are thickness fringes.

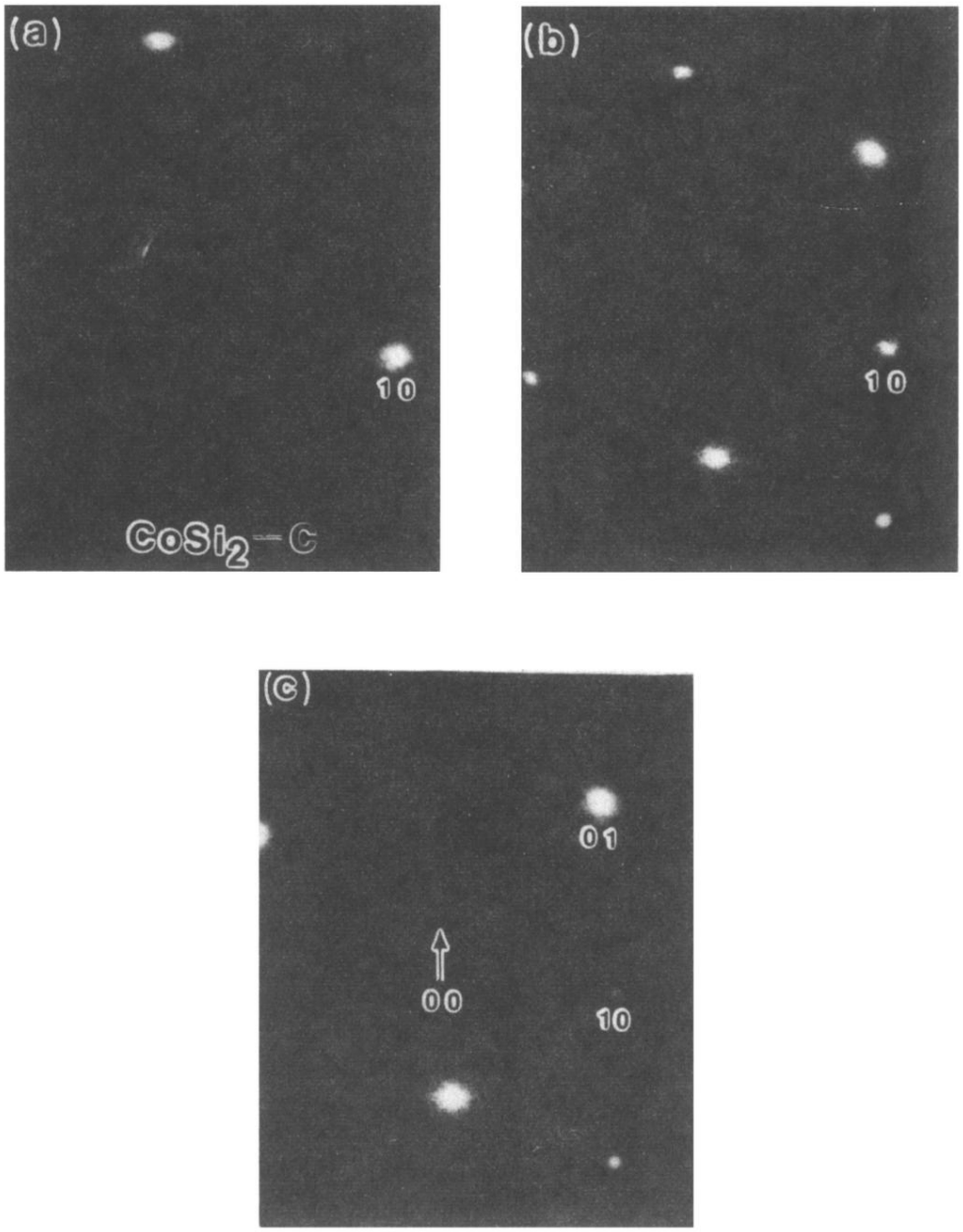

FIG. 3. LEED patterns for the $CoSi_2$-*C* surface at various energies. (a) 57 eV, (b) 79 eV, (c) 86 eV.

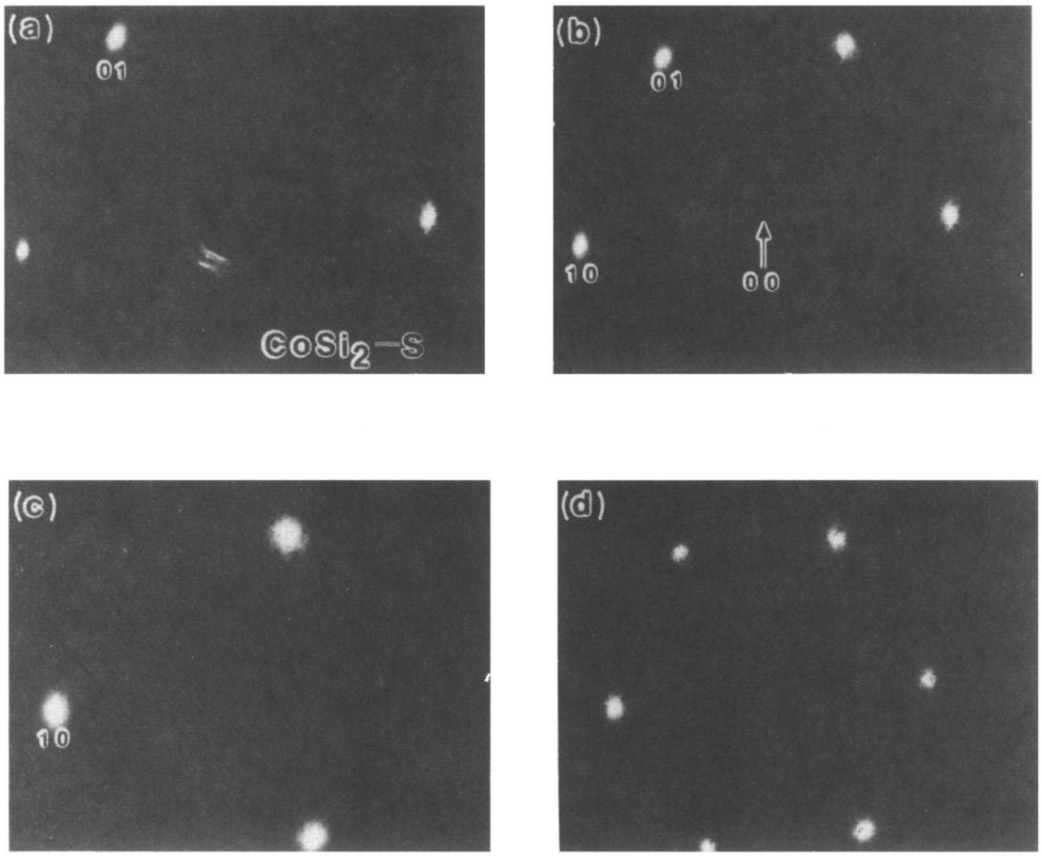

FIG. 4. LEED patterns for the $CoSi_2$-*S* surface at various energies. (a) 46 eV, (b) 58 eV, (c) 80 eV, (d) 88 eV.

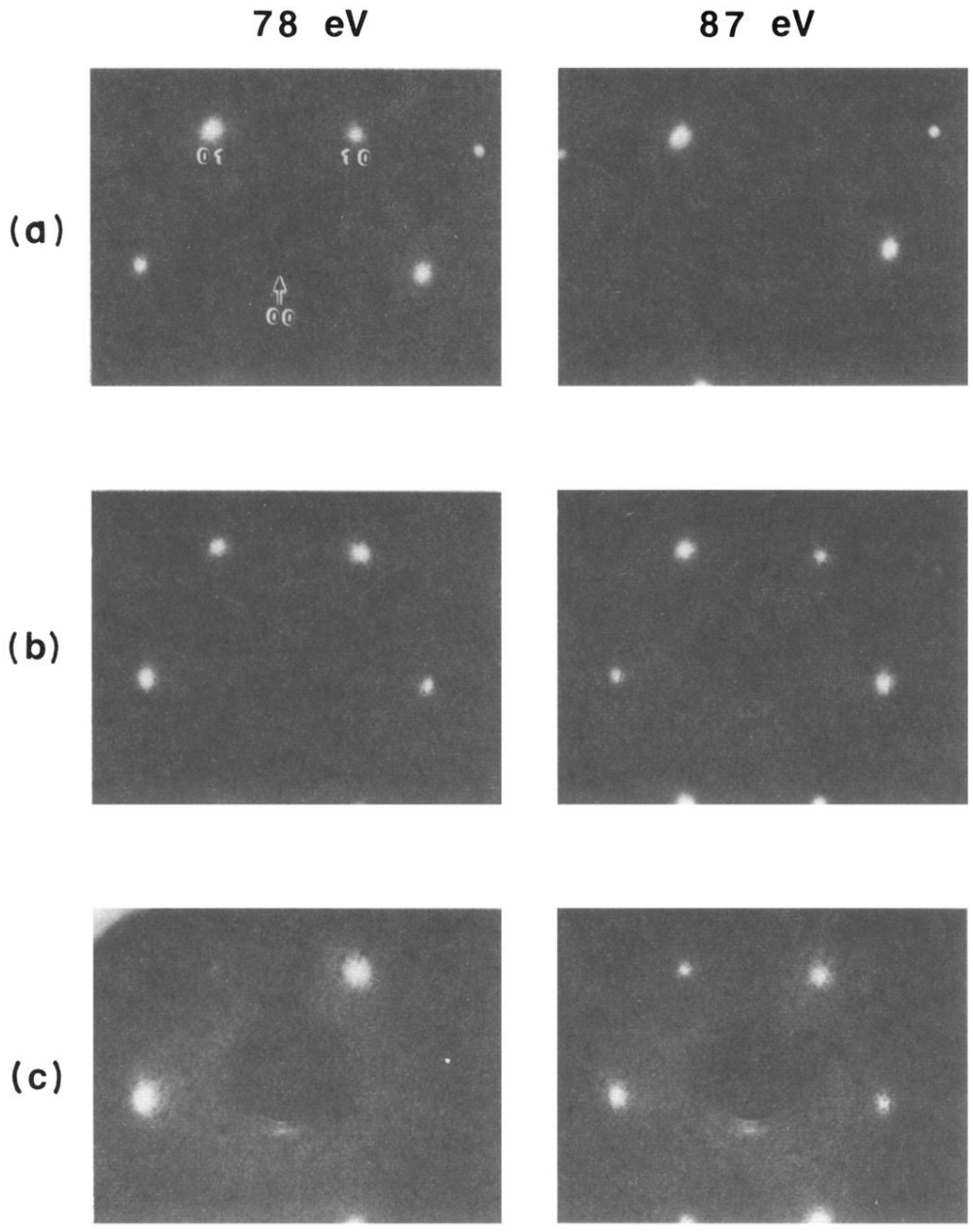

FIG. 5. LEED patterns for (a) $CoSi_2$-*C* surface (b) with one monolayer and (c) with two monolayers of Si deposited over and not annealed. Characteristic energies of the $CoSi_2$-*S* and $CoSi_2$-*C* surfaces (78 and 87 eV) are shown for each.

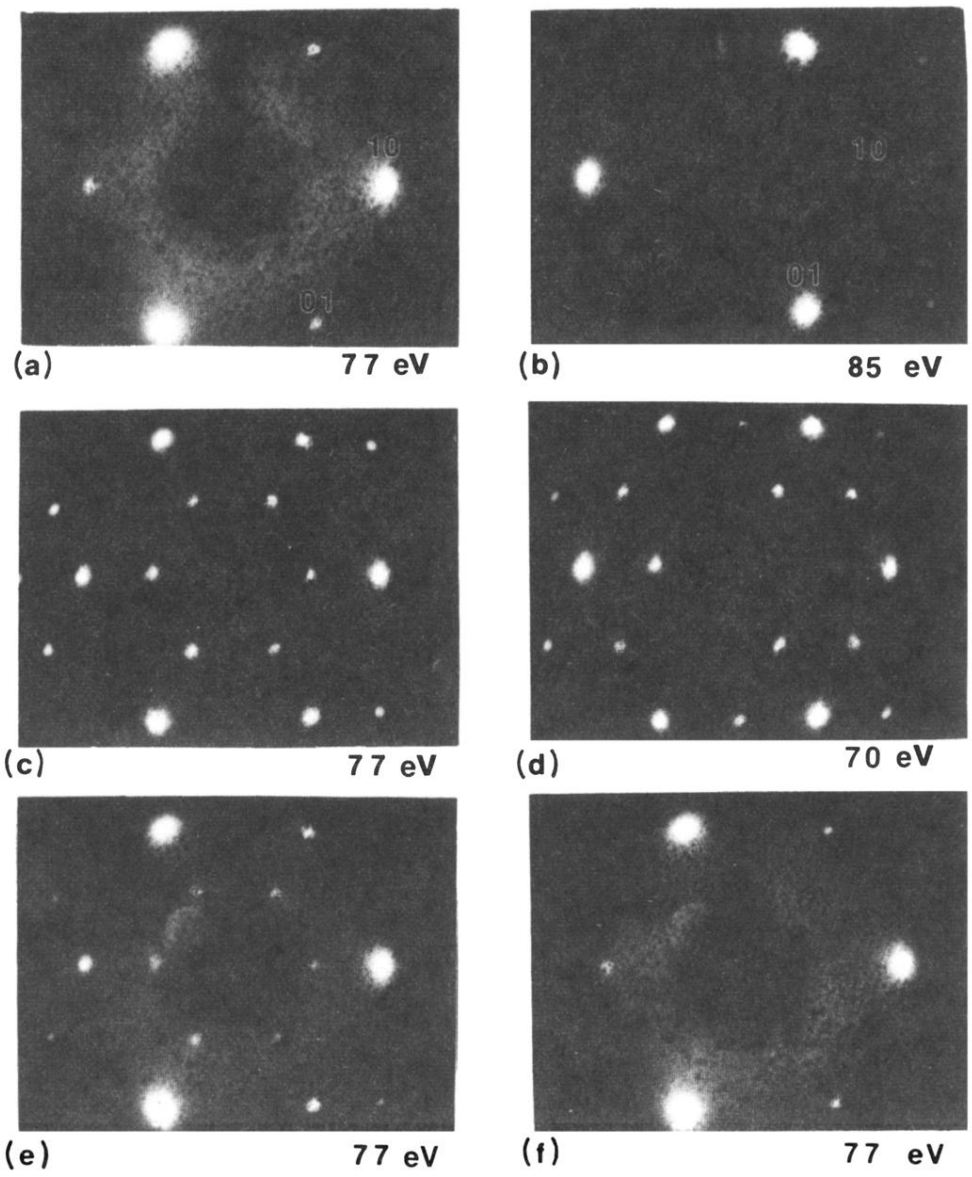

FIG. 6. LEED patterns of the $CoSi_2$ surface taken in a single deposition and annealing sequence. Voltages are as shown. (a) Silicide substrate showing strong threefold symmetry characteristic of single-crystal, epitaxial, type-*B* silicide after annealing at 580 °C for 1 min ($CoSi_2$-*S* surface). (b)–(f) show surface with 2 Å Co overlayer. (b) Annealed at 450 °C for 1 min. LEED pattern is typical of $CoSi_2$-*C* surface. (c) and (d) Annealed at 450 °C for 18 min. Patterns show 2×2 plus sixfold 1×1 symmetry. (e) Annealed at 480 °C for 9 min. Pattern shows weak 2×2 plus primarily threefold 1×1 symmetry. (f) Annealed at 590 °C for 30 sec. The LEED pattern is again typical of the $CoSi_2$-*S* surface.